NMR Experiments for the Study of Photointermediates: Application to the Photoactive Yellow Protein

Gilles Rubinstenn,[1] Geerten W. Vuister,[2] Nico Zwanenburg, Klaas J. Hellingwerf,[3] Rolf Boelens, and Robert Kaptein[4]

Bijvoet Center for Biomolecular Research, Utrecht University, Padualaan 8, 3584 CH Utrecht, The Netherlands

Many biological processes involve the interaction of light with the living cell. Examples are photosynthesis, phototaxis, photorepair of DNA damage, and the process of vision. In all these cases proteins or protein complexes serve as the primary photoreceptors and invariably these receptors cycle through a number of intermediate states and are regenerated at the end of the cycle. Turnover kinetics usually preclude the detailed solution study of these photocycle intermediates. Here, we present an approach that enables the NMR study of the blue-shifted intermediate pB in the photocycle of photoactive yellow protein (PYP) (*1–4*). PYP, a 14-kDa water-soluble protein, has been proposed to be a photosensor for the negative phototactic response toward the intense blue light of *Ectothiorhodospira halophila* (*5*), a motile bacterium which survives in Egyptian salt lakes. Light excitation induces a series of structural and dynamic changes yielding a blue-shifted, long-lived intermediate pB with a lifetime on the order of 1 s (cf., Fig. 1). This photocycle is triggered by the *trans/cis* isomerization (*6*) of the chromophore double bond (*7, 8*). This kinetic intermediate is generated using argon light irradiation inside the NMR probe, while its properties are studied by multidimensional heteronuclear experiments. Assignment of the resonances of pB was obtained by using a 2D ^{1}H–^{15}N correlation experiment in analogy to a previously proposed ^{1}H NMR experiment for spin coherence transfer in chemical reactions (SCOTCH) (*9*). The results of this study show that pB is structurally disordered and exists as a family of conformers in exchange on a millisecond timescale.

EXPERIMENTAL PROCEDURES

Uniformly ^{15}N-labeled PYP was prepared as described before (*10*). Samples consisted of a 0.6 mM solution of PYP in 95:5 v:v $H_2O:D_2O$ at pH 5.75 in 50 mM deuterated acetate buffer, and a protease inhibitor cocktail (1 mM pefablock, 5 μM leupepsin, 1 mM EDTA). A total sample volume of 300 μl was inserted into a Shigemi tube (Shigemi, Inc., Allison Park, PA). Subsequently, the distance between the bottom of the tube and the internal glass sliding piston was adjusted to 15.5 mm. The rather low concentration and short sample height are imposed by the high extinction coefficient of the ground state pG in order to obtain efficient irradiation conditions.

The setup for the excitation of the ground state of PYP inside the NMR magnet is depicted in Fig. 2. A Stabilite 2017 Argon laser (Spectra-Physics Lasers Inc., Darmstadt, Germany) was used as a light source. The multiline laser beam was directed into a Fibropsil quartz fiber ($\varnothing$ 400 μm, Quartz & Fibres, Pithiviers, France) via a refocusing lens. The free edge of the fiber was inserted in the glass piston of a Shigemi tube. The 7-mm-long end scattered the light beam into the sample. The irradiation was controlled by a focal plane shutter that was placed between the light source and the lens. The power yield of this setup equals approximately 25% (in the following discussion the indicated power levels will be the laser outputs). The Shigemi tube and fiber were inserted into the NMR magnet in the usual way.

The NMR experiments were recorded at 38°C using a Varian Unity/*Inova* operating at 499.91 ^{1}H resonance frequency, equipped with a triple-resonance probehead and a shielded *z*-gradient coil. Data were processed using the NMRPipe software package (*11*) and analyzed using REGINE (*12*).

RESULTS AND DISCUSSION

The intensity and length of the light pulse necessary to achieve the conversion of the pG state of PYP into the pB state were first calibrated by monitoring the disappearance of the low-field methyl resonance of alanine 67 (−0.82 ppm) in the 1D spectrum (*10*). The limiting factors were the lower stability of PYP in the presence of light and the need to maintain a reasonable sample homogeneity. Whereas a sample of PYP in the absence of light excitation is stable for weeks at 38°C and does not require any special protection against proteolysis, PYP quickly decays under irradiation conditions. A continuous

---
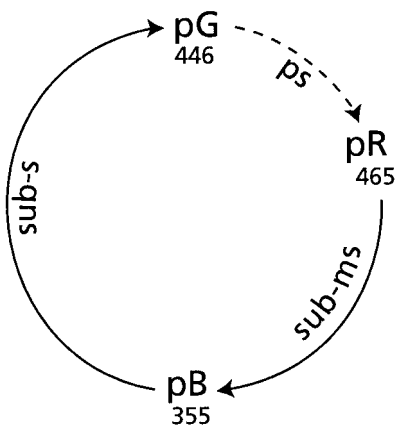
FIG. 1. Photocycle of the photoactive yellow protein. pG is the ground state, pR the red-shifted intermediate, and pB the blue-shifted intermediate. The absorption maximum, λ_{max} (in nm), is indicated for the three states.

light irradiation of 0.4 W induced complete degradation of the sample in only a few hours. This degradation was identified as a proteolysis of the 30 N-terminal amino acids. Subsequently, we observed that the sample could stand higher power levels of irradiation upon addition of a protease inhibitor cocktail. In this case, provided that overheating of the sample was avoided by interleaving light excitations (0.3–0.7 s) and dark periods ($>$1.5 s), relatively higher power levels could be used (up to 2 W) for more than 3 weeks without any degradation. The irradiation of the sample also induces a temperature gradient along the z axis, estimated to be 2°C over the length of the RF coil. The resulting inhomogeneity of the axial shims could easily be accommodated by shimming of the sample under irradiating conditions. No overall heating effect was observed. Under optimal conditions, an irradiation of 400 ms duration using 1.75 W of laser power, followed by acquisition under light conditions (150 ms), achieved 95% conversion of pG into pB. We also checked that a 2-s delay was sufficient to recover over 90% of the PYP back in the pG state.

In order to verify that our experimental setup was indeed converting the ground state pG of PYP into the long-lived state pB, we looked at the changes induced in the UV spectrum of a slightly less concentrated solution (0.2 mM) of PYP under the same conditions of pH, buffer, and temperature. By increasing the light intensity a gradual transformation of pG, λ_{max} = 446 nm (1), into pB, λ_{max} = 355 nm (13), is induced.

The general scheme for recording the NMR experiments is shown in Fig. 3A. A dark and a light spectrum are recorded in a scan-by-scan interleaved way. Approximately 350 ms before the end of the relaxation delay the laser excitation is switched on and is kept on during the pulse sequence and the acquisition time. The dark experiment is recorded in the absence of any light irradiation and the resulting dark spectrum of PYP constitutes a control spectrum as it is recorded under experimental conditions identical to those used for the spectrum of the excited PYP. This enables a quantitative comparison of peak

intensities and lineshapes as well as the monitoring of sample integrity. Modifications in the position, lineshape, and intensity of related cross peaks in the pG and pB spectra could therefore be fully attributed to changes in the structure and dynamics of PYP. The ^{15}N–^{1}H HSQC, ^{15}N-filtered TOCSY (14), ^{15}N-SCOTCH of pG and pB were recorded in this way with a full photocycle completed for each transient.

Once recorded, the ^{15}N–^{1}H HSQC of pB had to be assigned. We designed a pulse sequence, shown in Fig. 3B, that correlates the ^{15}N chemical shift of the pG state with the ^{1}H chemical shift of the ^{15}N attached protons of the pB state for each ^{15}N–^{1}H spin pair. In analogy to the ^{1}H experiment for the transfer of spin coherence (SCOTCH) (9), we propose naming this experiment ^{15}N-SCOTCH. It employs the possibility of converting pG into pB via a light pulse, the duration of which is of the order of the longitudinal relaxation time of nitrogen, and of recovering pG within a reasonable delay.
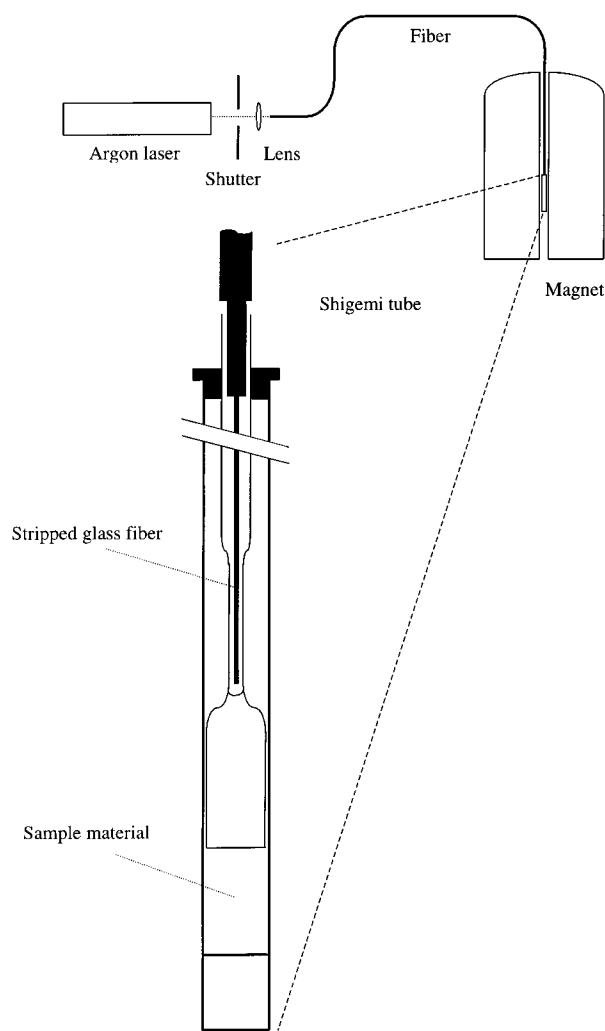
FIG. 2. Experimental setup for the NMR study of photocycle intermediates. The light from an argon laser is focused on a flexible light guide which is attached to a 5-mm Shigemi tube as shown.
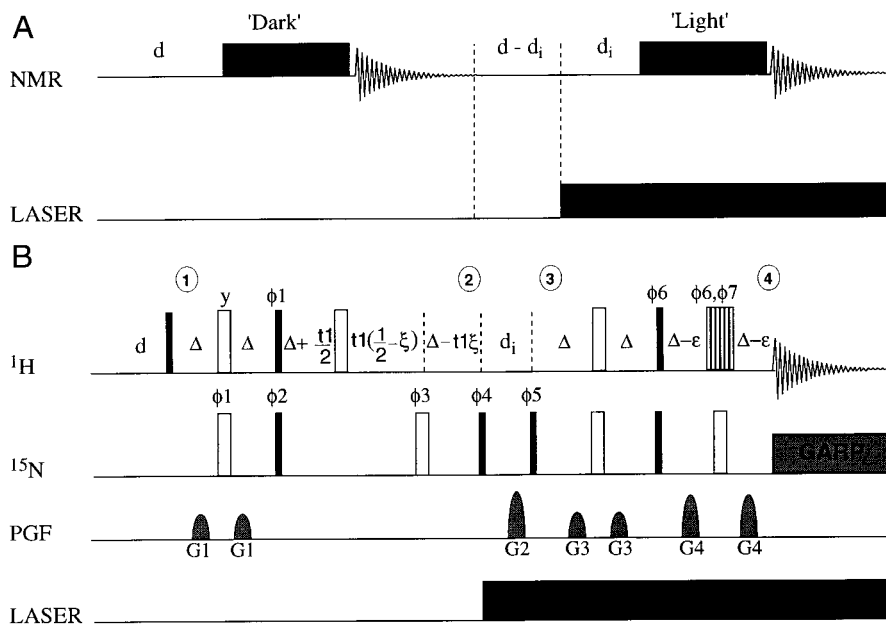
FIG. 3. General NMR scheme for the study of pB (A), ^{15}N-SCOTCH subsequence for HSQC assignment (B). The symbols used in A are defined in the text. Filled and unfilled boxes represent 90° and 180° hard pulses, respectively. Unless expressed otherwise, the phase of the pulses was x. $\phi1$ (y, $-y$); $\phi2$ (x)4 ($-x$)4; $\phi3$ (x)8 ($-x$)8; $\phi4$ (y); $\phi5$ (y)8 ($-y$)8; $\phi6$ (x)2 (y)2; $\phi7$ ($-x$)2 ($-y$)2; ϕrec (x, $-x$, y, $-y$, $-x$, x, $-y$, y, $-x$, x, $-y$, y, x, $-x$, y, $-y$). For each increment of $t1$, $\phi4$ and ϕrec were both incremented by 180° according to the STATES procedure; δ was set to 1.7 s. The power level of the light excitation was 1.75 W and d_i was set to 0.3 s. Δ was set to 2.7 ms. The semiconstant time delay ξ was given the maximum value such that the delay $\Delta - t1 \cdot \xi$ does not become negative. With a spectral width of 1852 Hz in D1 and 80 pairs of real–imaginary points recorded, this amounts to $\xi = 0.0625$. This decreases the semiconstant period by approximately 10%. The interpulse delay τ in the WATERGATE pulse train was set to 1.33 μs, and the correction ϵ for J evolution to $1.685 \cdot \tau = 224$ μs. Sine-shaped pulsed-field gradients were used to purge unwanted coherences. The following lengths and strengths were used: G1 (1 ms, 2 Gcm^{-1}), G2 (1 ms, 29 Gcm^{-1}), G3 (1 ms, 7 Gcm^{-1}), G4 (1.5 ms, 30 Gcm^{-1}). GARP decoupling employing an RF field strength of 2500 Hz was used during acquisition.. The proton spectral width was set to 6667 Hz and the nitrogen spectral width to 1852 Hz. The ^{1}H carrier was set at 4.75 ppm and the ^{15}N carrier at 116.5 ppm.; 160 real and imaginary FIDs of 2048 points were recorded.

The ^{15}N-SCOTCH experiment employs a refocused INEPT (15) in conjunction with semiconstant time frequency labeling (16) to transfer proton pG magnetization, I_y(pG), at time point 1 to nitrogen S_z(pG) magnetization of pG at time point 2, where I and S denote the ^{1}H and ^{15}N spin operators (17), respectively. During time $\tau1$ the pG ^{15}N magnetization is labeled with its chemical shift.

During the delay d_i (300 ms), in the presence of light irradiation, S_z(pG) is partially converted at time point 3 into S_z(pB). Both S_z(pG) and S_z(pB) are transferred into observable proton magnetization, I_y(pG) and I_y(pB), at time point 4 by the reverse INEPT sequence in which the last ^{1}H 180° pulse has been replaced by a 3—9—19—19—9—3 WATERGATE pulse train (18). At the experimental parameters chosen, pB was populated for 85%. Note that the two terms S_z(pG) (15%) and S_z(pB) (85%) also contain an attenuation coefficient, due to relaxation. About 40% of the overall magnetization is thus lost, assuming an identical rotational correlation time of 6 ns and identical ^{15}N longitudinal relaxation rates for the dark and the light states (10).

This experiment results in a ^{1}H–^{15}N correlation spectrum with cross peaks at the ^{15}N chemical shift of pG and the ^{1}H chemical shift of pB for each amide bond of the backbone of

PYP, together with residual cross peaks of the ground state pG. As can be seen in Fig. 4, this enables the assignment of the cross peaks of the HSQC of pB by starting from the corresponding peaks in the spectra of pG and pB and by connecting them by means of the exchange spectrum correlations. Using this strategy 67 of 116 amide cross peaks in the pG spectrum could be unambiguously related to their counterpart in the spectrum of pB. For the remaining 49 amide spin systems no cross peak was found in the HSQC of pB under the experimental conditions. In the HSQC of pB as well, no intense cross peaks at random coil positions were observed, which would be indicative of a fully unconstrained polypeptide backbone. Since the H$_2$O magnetization was kept close to its thermal equilibrium, avoiding the loss of cross peaks by saturation transfer, the lack of observed cross peaks in the HSQC of pB is likely to be a result of conformational exchange occurring on a millisecond timescale between multiple conformations of pB. This conclusion is further supported by the fact that the assigned pB cross peaks showed significant broadening of the resonance lines along the ^{15}N axis when compared to corresponding cross peaks of pG. In addition, substantial structural changes occur, as judged from the ^{15}N chemical shift differences between corresponding cross peaks in pB and pG, which
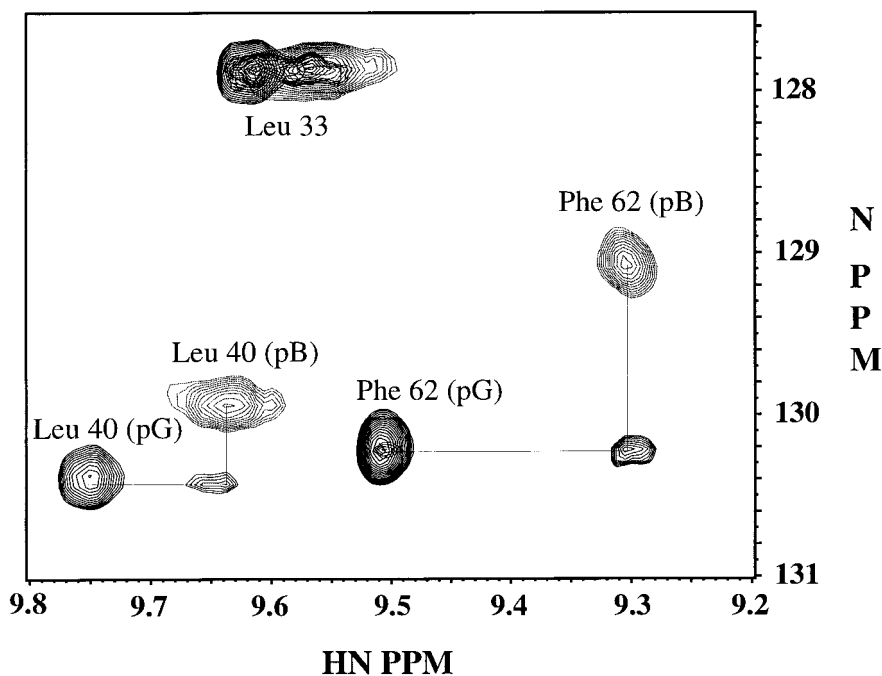
FIG. 4. Superimposed regions of the HSQC spectra of pG, pB, and the ^{15}N-SCOTCH exchange experiment connecting the HSQC cross peaks. The ^{15}N–^{1}H HSQC spectra of pG and pB were recorded using the general scheme of Fig. 3A. The light and dark ^{15}N–^{1}H HSQC employed gradient coherence selection, water flip-back, and sensitivity enhancement (*20*); *d* was set to 2 s. The power level of the light excitation was 1.75 W and d_i was set to 0.4 s. All other experimental parameters were as listed in the legend to Fig. 3. The ^{15}N-SCOTCH experiment was recorded by using the pulse sequence of Fig. 3B.

exhibit a pairwise rmsd of 2.15 ppm and a maximum deviation of 9 ppm. Earlier we showed how these data are highly indicative of the collapse of the hydrophobic core and a disruption of the central β-sheet of PYP (*19*).

A ^{15}N-filtered aromatic TOCSY experiment (*14*), recorded using the general interleaved setup of Fig. 3A, is also indicative of major changes and a disruption of the hydrophobic core of PYP (data not shown). Aromatic residues displaying only small differences in chemical shift are located in regions displaying only small changes in the backbone ^{15}N and ^{1}H chemical shifts. Conversely, large changes or the loss of cross peaks is observed for those residues also showing large effects in their backbone shifts.

We have designed a convenient setup that enables generation and observation by multidimensional NMR of the long-lived intermediate of the PYP photocycle. This approach could be applied to the study of any photocycle intermediate, provided that it exhibits reasonable conversion kinetics. We implemented the ^{15}N-SCOTCH principle in order to assign the resonance frequencies of the [15]N–[1]H spin vectors of the intermediate state. The differences between the HSQC spectra of pG and pB give evidence for dramatic dynamic differences and structural changes between the well-defined and rigid initial state (*10*) and the partially disordered and more flexible kinetic intermediate. The study of the recovery of the pG state from the pB states shows that the rates are inhomogeneous with respect to structure, which are likely correlated with the ener-

getic barriers in the refolding process. This method provides a unique approach for the solution study of the underlying molecular mechanisms involved in the phototactic response of *Ectothiohodospira halophila.*

REFERENCES

1. T. E. Meyer, *Biochim. Biophys. Acta* **806,** 175–183 (1985).

2. T. E. Meyer, J. C. Fitch, R. G. Bartsch, G. Tollin, and M. A. Cusanovich, *Biochim. Biophys. Acta* **1016,** 364–370 (1987).

3. D. E. McRee, J. A. Tainer, T. E. Meyer, J. Van Beeumen, M. A. Cusanovich, and E. Getzoff, *Proc. Natl. Acad. Sci. USA* **86,** 6533–6537 (1989).

4. G. E. O. Borgstahl, D. R. Williams, and E. D. Getzoff, *Biochemistry* **34,** 6278–6287 (1995).

5. W. W. Sprenger, W. D. Hoff, J. P. Armitage, and K. J. Hellingwerf, *J. Bacteriol.* **175,** 3096–3104 (1993).

6. R. Kort, H. Vonk, X. Xu, W. D. Hoff, W. Crielaard, and K. J. Hellingwerf, *FEBS Lett.* **382,** 73–78 (1996).

7. W. D. Hoff, I. H. M. van Stokkum, H. J. van Ramesdonk, M. E. van Brederode, A. M. Brouwer, J. C. Fitch, T. E. Meyer, R. van Grondelle, and K. J. Hellingwerf, *Biophys. J.* **67,** 1691–1705 (1994).

8. M. Baca, G. E. O. Borgstahl, M. Boissinot, P. M. Burke, D. R. Williams, K. A. Slater, and E. D. Getzoff, *Biochemistry* **33,** 14370–14377 (1994).

9. J. Kemmink, G. W. Vuister, R. Boelens, K. Dijkstra, and R. Kaptein, *J. Am. Chem. Soc.* **108,** 5631–5633 (1986).

10. P. E. Dux, G. Rubinstenn, G. W. Vuister, R. Boelens, E. A. A.

Mulder, K. A. Hård, W. D. Hoff, A. R. Kroon, W. Crielaard, K. J. Hellingwerf, and R. Kaptein, *Biochemistry* **37,** 12689–12699 (1998).

11. F. Delaglio, S. Grzesiek, G. W. Vuister, G. Zhu, J. Pfeifer, and A. Bax, *J. Biomol. NMR* **6,** 277–293 (1995).

12. G. J. Kleywegt, G. W. Vuister, A. Padilla, R. M. A. Knegtel, R. Boelens, and R. Kaptein, *J. Magn. Reson. B* **102,** 166–176 (1993).

13. W. D. Hoff, P. Düx, K. Hård, B. Devreese, I. M. Nutgeren-Roodzant, W. Crielaard, R. Boelens, R. Kaptein, J. Van Beeumen, and K. J. Hellingwerf, *Biochemistry* **33,** 13959–13962 (1994).

14. B. Whitehead, M. Tessari, P. Düx, R. Boelens, R. Kaptein, and G. W. Vuister, *J. Biomol. NMR* **9,** 313–316 (1997).

15. G. A. Morris and R. Freeman, *J. Am. Chem. Soc.* **101,** 760–762 (1979).

16. S. Grzesiek and A. Bax, *J. Biomol. NMR* **3,** 185–204 (1993).

17. O. W. Sørensen, G. W. Eich, M. H. Levitt, G. Bodenhausen, and R. R. Ernst, *Prog. NMR Spectrosc.* **16,** 163–164 (1983).

18. M. Piotto, V. Saudek, and V. Sklenar, *J. Biomol. NMR* **2,** 661–665 (1992).

19. G. Rubinstenn, G. W. Vuister, F. A. A. Mulder, P. E. Düx, R. Boelens, K. J. Hellingwerf, and R. Kaptein, *Nature Struct. Biol.* **5,** 568–570 (1998).

20. L. E. Kay, P. Keifer, and T. Saarinen, *J. Am. Chem. Soc.* **114,** 12593–12595 (1992).

21. J. P. Armitage, *Can. J. Microbiol.* **34,** 475–481 (1988).